J Solid State Electrochem (2012) 16:673–679
DOI 10.1007/s10008-011-1407-7

ORIGINAL PAPER

Properties of $LiNiO_2$ cathode and graphite anode in *N*-methyl-*N*-propylpyrrolidinium bis (trifluoromethanesulfonyl)imide

Agnieszka Swiderska-Mocek · Andrzej Lewandowski · Beata Kurc

Received: 17 February 2011 / Revised: 4 April 2011 / Accepted: 16 April 2011 / Published online: 4 May 2011

Abstract Electrochemical properties of $LiNiO_2$|Li and $LiNiO_2$|graphite cells were analysed in ionic liquid electrolyte $[Li^+][MePrPyrr^+][NTf_2^-]$ (based on *N*-methyl-*N*-propylpyrrolidinium bis(trifluoromethanesulphonyl)imide, $[MePrPyrr^+][NTf_2^-]$) using impedance spectroscopy and galvanostatic techniques. The ionic liquid is incapable of protective solid electrolyte interface (SEI) formation on metallic lithium or lithiated graphite. However, after addition of VC, the protective coating is formed, facilitating a proper work of the Li-ion cell. Scanning electron microscopy images of pristine electrodes and those taken after electrochemical cycling showed changes which may be interpreted as a result of SEI formation. The charging/discharging capacity of the $LiNiO_2$ cathode is between 195 and 170 mAh g^{-1}, depending on the rate. The charging/discharging efficiency of the graphite anode drops after 50 cycles from an initial value of ca. 360 mAh g^{-1} to stabilise at 340 mAh g^{-1}. The replacement of a classical electrolyte in molecular liquids (cyclic carbonates) with an electrolyte based on the MePrPyrrNTf$_2$ ionic liquid highly increases in the cathode/electrolyte non-flammability.

Keywords Ionic liquid · Lithium · $LiNiO_2$ · Lithium-ion battery · Cathode · SEI

A. Swiderska-Mocek (✉) · A. Lewandowski · B. Kurc
Faculty of Chemical Technology,
Poznań University of Technology,
60-965 Poznań, Poland
e-mail: agnieszka.swiderska-mocek@put.poznan.pl

Introduction

Lithium-ion batteries are typically composed of a carbon anode, $LiMn_2O_4$ or $LiCoO_2$ cathode and $LiPF_6$ solution in a mixture of cyclic carbonates serving as an electrolyte. Both electrodes corrode in electrolytes forming passivation films. The formed insoluble passivation layer, usually called solid electrolyte interface (SEI), should (1) conduct Li^+ ions, (2) protect electrodes from their further corrosion and (3) facilitate charge transfer reaction at the solid SEI/electrode interface. At high voltage differences (overcharging) or during contact with air (battery damage), the reaction of electrodes, especially the anode with the environment (solvent, moisture), may result in system ignition. Instead of volatile cyclic carbonates, non-volatile room temperature ionic liquids (RTILs) may be applied as lithium salt solvents [1–5]. In molten salts, including RTILs, strong Coulomb interactions between ions counterbalance the thermal energy, and the resulting equilibrium leads to low vapour pressure making RTILs practically non-flammable [6–12]. Among RTILs, those based on *N*-methyl-*N*-propylpiperidinium, $[MePrPip^+]$, and *N*-alkyl-*N*-methylpyrrolidinium $[RMePyrr^+]$ cations and bis(trifluoromethanesulphonyl)imide anion, $[NTf_2^-]$ seem to be promising solvents for lithium salts. It is observed that the $[Li^+][MePrPyrr^+][NTf_2^-]$ electrolyte was compatible with $LiCoO_2$, $LiFePO_4$ and $LiMn_2O_4$ cathodes [13–18], as well as with such anode materials as graphite, hard carbon, S and tin–carbon composite [19–24]. The general aim of this paper was to study the $LiNiO_2$ cathode in the $[Li^+][MePrPyrr^+][NTf_2^-]$ ionic liquid electrolyte, which is characterised by a relatively low potential (3.8 V versus Li), though a high specific capacity (220 mAh g^{-1} [25]). Such a cathode may be a part of a safe cell working with the graphite anode and the ionic liquid electrolyte.

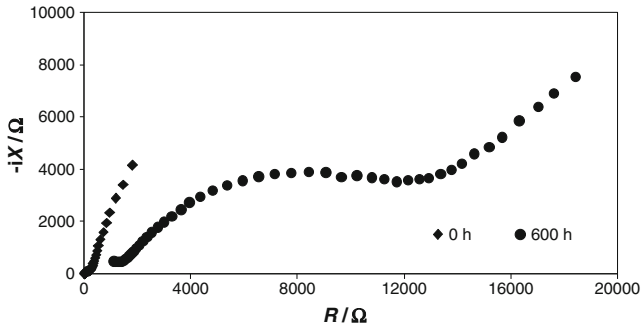

Fig. 1 Impedance plots for unsymmetrical $LiNiO_2$|0.7 M $LiNTf_2$ in $MePrPyrrNTf_2$| Li cell kept under open circuit conditions as a function of time

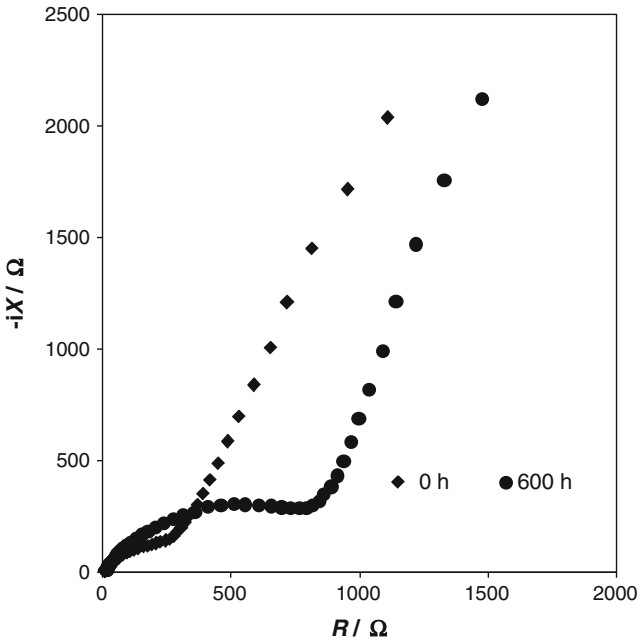

Fig. 3 Impedance plots for the unsymmetrical $LiNiO_2$|0.7 M $LiNTf_2$ in $MePrPyrrNTf_2$+10% VC|Li cell kept under open circuit conditions as a function of time

Experimental

Materials

$LiNiO_2$ powder (Aldrich), graphite SL-20 (G, Superior Graphite, USA) and KS-15 (G) (Lonza), carbon black (CB, Fluka), poly(vinylidene fluoride) (PVdF, Fluka), vinylene carbonate (VC, Aldrich), lithium foil (0.75 mm thick, Aldrich) and lithium bis(trifluoromethanesulphonyl)imide ($LiNTf_2$, Fluka) were used as received. *N*-methyl-*N*-propylpyrrolidinium bis(trifluoromethanesulphonyl)imide ($[MePrPyrr^+][NTf_2^-]$) was prepared according to the literature [24], by reacting *N*-methylpyrrolidinium (Aldrich) with propylbromide (Aldrich) followed by metathesis with lithium bis(trifluoromethanesulphonyl)imide. Ionic liquid $[Li^+][MePrPyrr^+][NTf_2^-]$ was obtained by dissolution of solid $LiNTf_2$ in liquid $[MePrPyrr^+][NTf_2^-]$ (0.7 M solution of $LiNTf_2$ in $[MePrPyrr^+][NTf_2^-]$). The cathode was prepared by casting a slurry of $LiNiO_2$, graphite KS-15 and PVdF (ratio 85:5:10) in *N*-methyl-2-pyrrolidone (NMP, Fluka) on a golden current collector (12 mm radius). Carbon electrodes were prepared on a copper foil (Hohsen, Japan) by the casting technique, from a slurry of graphite SL-20 (G), carbon black (CB) and PVdF in *N*-methyl-2-pyrrolidone (NMP, Fluka). The ratio of components (G):(CB):(PVdF) was 85:5:10 (by weight). The layers of electrodes were formed by evaporation of the solvent (NMP) at 120 °C in vacuum.

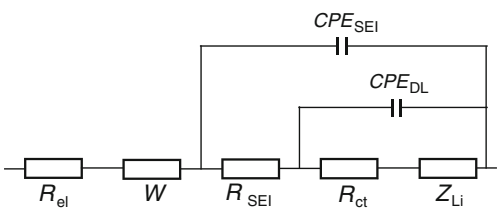

Fig. 2 An equivalent circuit representing the electrolyte/electrode system

Measurements

Cycling efficiency of the cathode was measured in a two-compartment cell against a counter electrode consisting of the lithium foil, separated by the glass microfibre GF/A separator (Whatman) and placed in an adapted 0.5″ Swagelok® connecting tube. The cycling measurements were taken using the ATLAS 0461 MBI multichannel electrochemical system (Atlas-Sollich, Poland). Galvanostatic charging/discharging of the $LiNiO_2$|Li and $LiNiO_2$|graphite cells were conducted between 3.2–4.2 and 2.5–4.2 V, respectively. The charging and discharging rates were C/10, C/5, C/3 and C/2. Always, the discharge rate was the same as charging rate. Interface resistance at the electrode/electrolyte interface was measured using an ac impedance analyzer (Atlas-Sollich system, Poland). Flash point of $[Li^+][MePrPyrr^+][NTf_2^-]$ was measured using an open-cup home-made apparatus, based on the Cleveland instrument, with a 1.5-ml cup. The cup was heated electrically through a sand bath, and temperature was measured using the M-3850 Metex (Korea) digital thermometer. The apparatus was scaled with a number of compounds of known flash points [24]. The surface of $LiNiO_2$ was estimated from the nitrogen adsorption BET isotherm using the ASAP2010 (Micromeritics, USA).

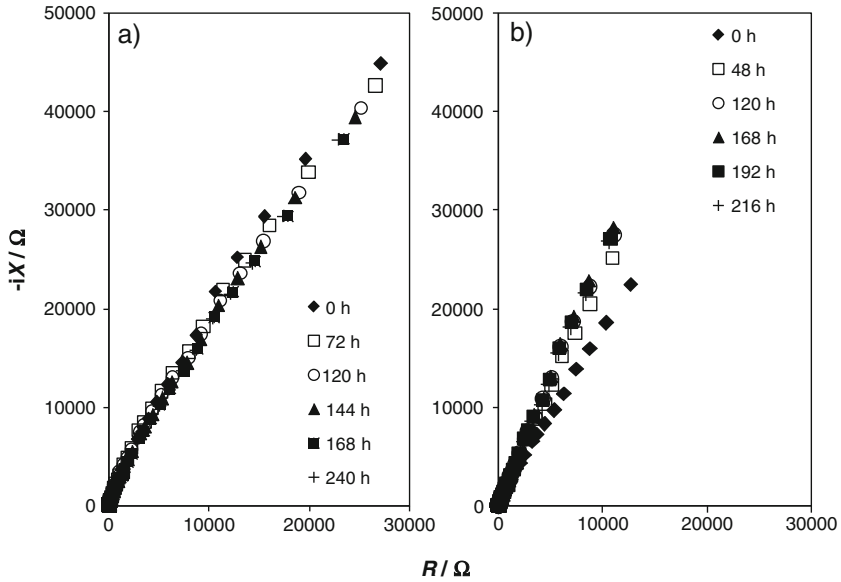

Fig. 4 Impedance plots for the symmetrical $LiNiO_2$|0.7 M $LiNTf_2$ in $MePrPyrrNTf_2$ | $LiNiO_2$ cell (**a** without VC, **b** containing 10 wt.% VC) kept under open circuit conditions as a function of time

Particle size was measured with the Zetasizer Nano ZS (Malvern Instruments Ltd.). After electrochemical measurements, cells were disassembled, and electrodes washed with DMC and dried in vacuum at room temperature. Scanning electron microscopy (SEM) as well as energy dispersive spectroscopy (EDX) of electrodes was done with a Tescan Vega 5153 apparatus. All operations were made in a dry argon atmosphere in a glove box.

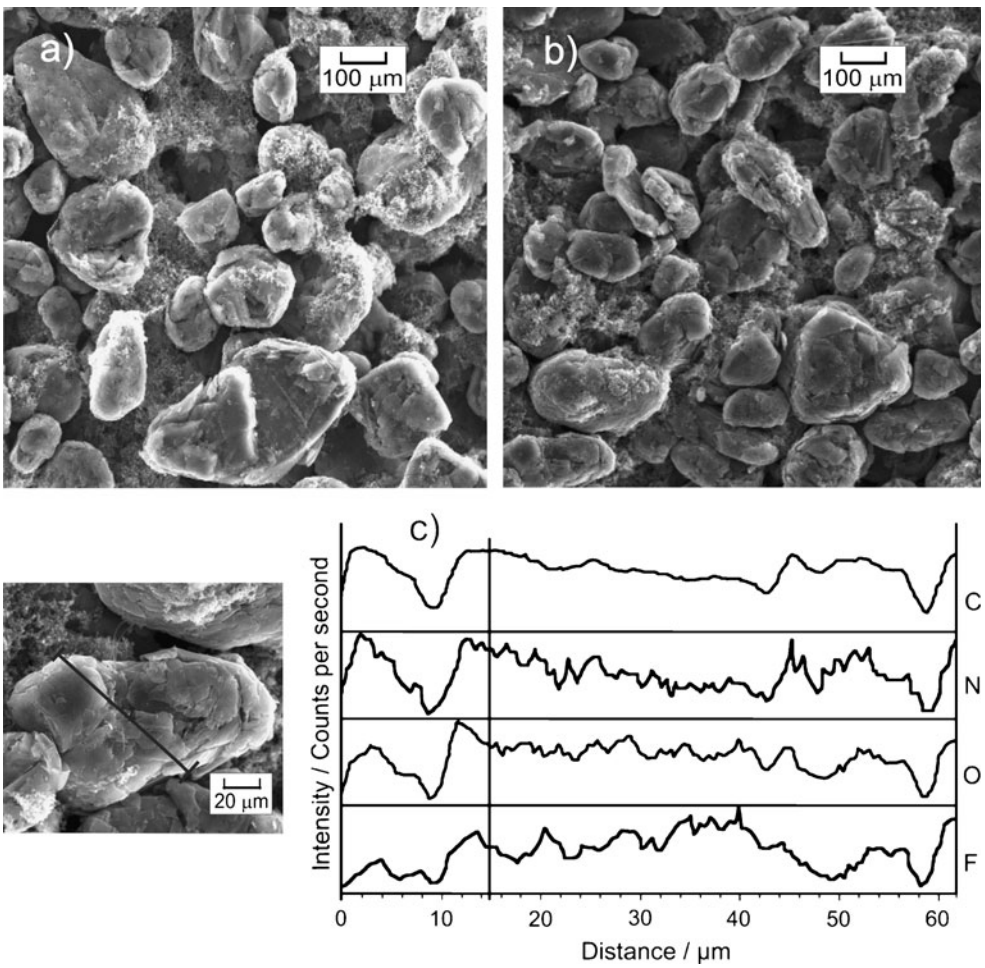

Fig. 5 SEM images of graphite anodes. **a** Pristine. **b**, **c** After seventh charge/discharge cycles. **c** EDX analysis of the cycled anode. Electrolyte 0.7 M $LiNTf_2$ in $MePrPyrrNTf_2$+VC wt.10%

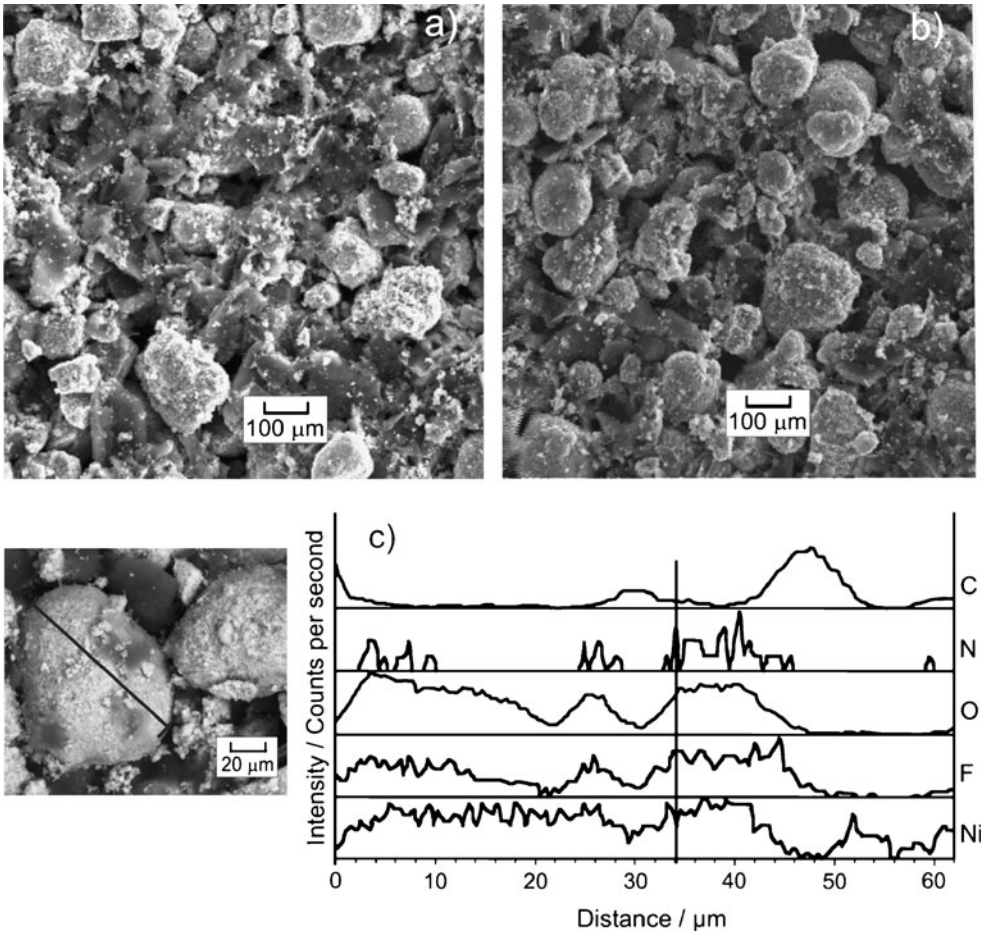

Fig. 6 SEM images of the $LiNiO_2$ cathode. **a** Pristine electrode. **b**, **c** After 15th charge/discharge cycles. **c** EDX analysis of the cycled anode. Electrolyte 0.7 M $LiNTf_2$ in $MePrPyrrNTf_2$+VC wt.10%

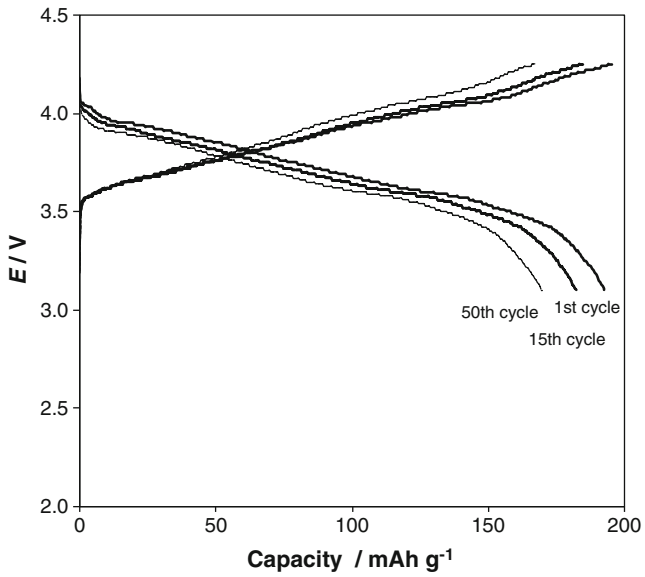

Fig. 7 Galvanostatic charging/discharging of the $LiNiO_2$|0.7 M $LiNTf_2$ in $MePrPyrrNTf_2$+10% VC|Li cell. $LiNiO_2$ mass in the cathode 2.7 mg. Current 22 mA/g (C/10)

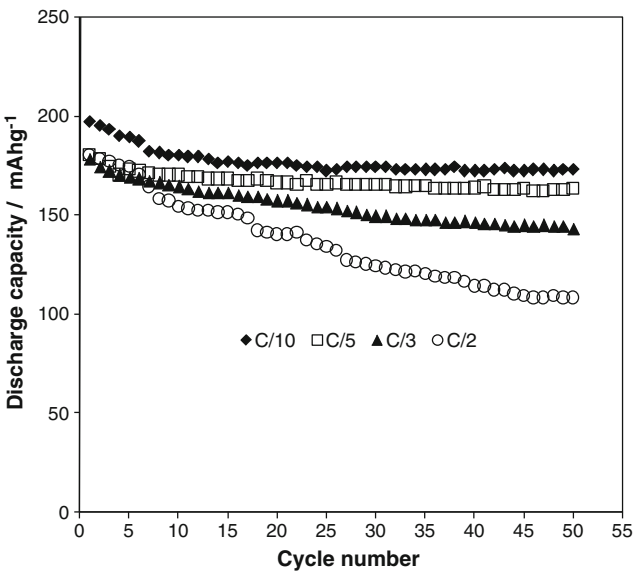

Fig. 8 Discharging capacity of the $LiNiO_2$|0.7 M $LiNTf_2$ in $MePrPyrrNTf_2$+10% VC|Li cell at various discharging rates

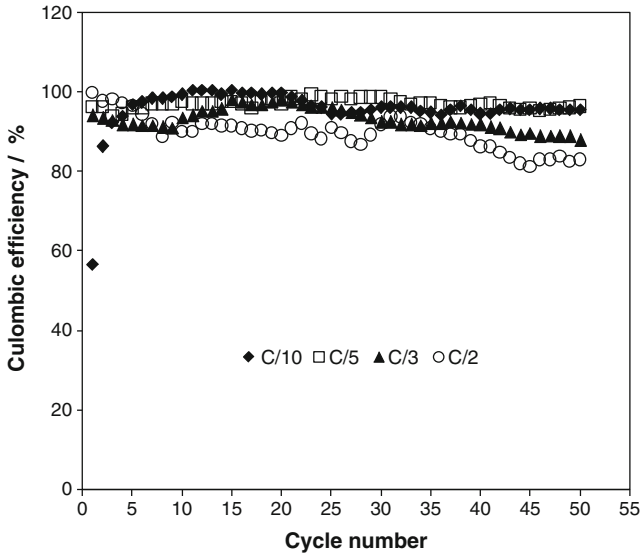

Fig. 9 Coulombic efficiency of the $LiNiO_2$|0.7 M $LiNTf_2$ in $MePrPyrrNTf_2$+10% VC|Li cell at various discharging rates

Results and discussion

SEI formation

Figure 1 shows the evolution of impedance of the $LiNiO_2$|0.7 M $LiNTf_2$ in $MePrPyrrNTf_2$|Li cell kept under the open circuit condition. It can be seen that cell resistance increases with time. Deconvolution of the impedance spectra was performed according to an equivalent circuit (Fig. 2). This consisted of an electrolyte (R_{el}), SEI (R_{SEI}) and charge transfer (R_{ct}) resistances in series with electrolyte and SEI Warburg impedance (W) as well as impedance Z_{Li} due to diffusion of lithium in $LiNiO_2$. Capacity of SEI and double-layer (between SEI and the electrode) are represented by constant phase elements parallel to R_{SEI}, R_{ct} and Z_{Li}. However, values of $R_{ct}+Z_{Li}$ cannot be separated into single contributions. The SEI resistance is 1.3 Ω immediately after the cell assembling, to increase to ca. 10 kΩ within 25 days (ca. 600 h). However, an addition of VC into the electrolyte prevents the cell from corrosion processes, due to SEI formation (Fig. 3); the initial R_{SEI} value is 30 Ω and increases to ca. 200 Ω after 600 h. It was shown in a previous publication [24] that impedance of a symmetrical Li|0.7 M $LiNTf_2$ in $MePrPyrrNTf_2$|Li cell increased by ca. three orders of magnitude within 36 days. Corrosion products do not protect the lithium electrode, but increase resistance. Impedance of a symmetrical $LiNiO_2$|0.7 M $LiNTf_2$ in $MePrPyrrNTf_2$|$LiNiO_2$ cell (with or without VC, Fig. 4) does not increase with time. This suggests that a potential corrosion of the anode (metallic lithium in laboratory test cells or graphite in complete cells [24]) is a key factor. Figures 5 and 6 show scanning electron microscopy (SEM) images of pristine electrodes (Fig. 5a and 6a) and after electrochemical cycling (Fig. 5b, c and 6b, c). Pristine graphite particles (Fig. 5a) are flat platelets with round edges after cycling, which may be interpreted as a result of SEI formation. No graphite exfoliation can be seen. The $LiNiO_2$ cathode after its electrochemical cycling (Fig. 6b, c) is also covered with a film and small aggregates. This 'micro-roughness' may indicate the formation of SEI layer [26–30]. The EDX analysis suggests that fluorine is present on electrodes surface (from electrochemical decomposition of NTf_2 anion).

Charging/discharging

Charging/discharging curves for the $LiNiO_2$|0.7 M $LiNTf_2$ in $MePrPyrrNTf_2$+10% VC|Li cell are shown in Fig. 7. The charging and discharging (Fig. 8) capacity of the $LiNiO_2$ cathode was between 195 and 170 mAh g^{-1} for lower rates (C/10, C/5). This value may be compared to the capacity found for cells working with classical electrolytes. A capacity of 180 mAh g^{-1} was obtained at low rates (C/20) [31] in the $LiAsF_6$ electrolyte and 155 mAh g^{-1} in the $LiPF_6$ solution in EC+DEC (7.5 mAh g^{-1}; C/30 rate) [32, 33]. A higher capacity (200 mAh g^{-1}) was reported for a system working with a 1-M $LiPF_6$ solution in a mixture of PC with 1,2-dimethoxyethane [34].

Properties of the $LiNiO_2$ cathode were reviewed [35, 36]. The cathode was described as having a practical capacity of only 100–120 mAh g^{-1} at high cycle numbers. Here, Coulombic efficiency (discharging capacity/charging capacity×100%) of the discharging process was found to be

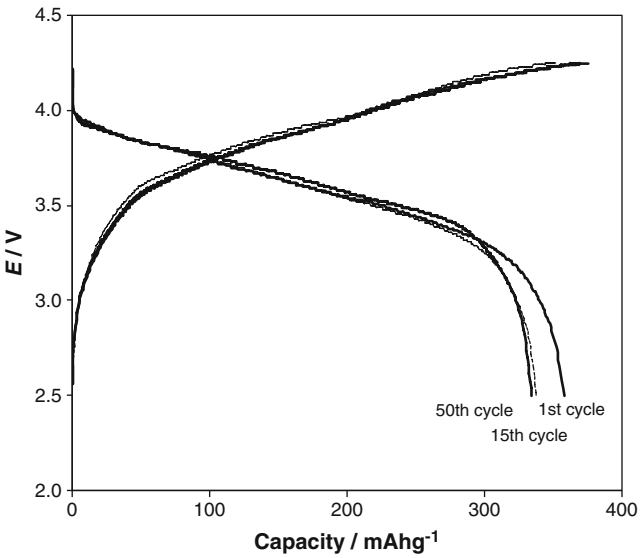

Fig. 10 Galvanostatic charging/discharging of the $LiNiO_2$|0.7 M $LiNTf_2$ in $MePrPyrrNTf_2$+10% VC|graphite cell. $LiNiO_2$ mass in the cathode 8.3 mg and graphite mass in the anode 4.1 mg. Current 18.5 mA/g (C/20)

close to 90–95% (±5%), depending on the discharge rate (Fig. 9). However, it can be see that in the case of the lowest C/10 rate, the initial Coulombic capacity increased considerably from ca. 60% up to 90–95%. This may be due to slow SEI formation during first three cycles.

Charging/discharging curves of a complete $LiNiO_2$|0.7 M $LiNTf_2$ in $MePrPyrrNTf_2$ + 10% VC|graphite Li-ion cell (at the *C*/20 rate) are shown in Fig. 10. The discharging efficiency after 50 cycles drops from an initial value of ca. 360 mAh g^{-1} to stabilise at 340 mAh g^{-1} (expressed versus the mass of graphite). The rate of charging/discharging is limited by lithium diffusion in the solid $LiNiO_2$ cathode (specific surface of 2.6 m^2 g^{-1}, particle size between 800 and 1,400 nm). The $R_{ct}+Z_{Li}$ value detected from deconvolution of impedance plots for the symmetrical $LiNiO_2$|0.7 M $LiNTf_2$ in $MePrPyrrNTf_2$|$LiNiO_2$ cell (Fig. 4) is ca. 10^5 Ω for the electrolyte both with and without VC and for an electrode mass of ca. 3 mg. Therefore, the cathode surface is (2.6 10^4 cm^2 g^{-1}) × (3 10^{-3} g)=78 cm^2. The current density approximated from the $R_{ct}+Z_{Li}$ value is j=(0.026 V/(10^5 Ω × 78 cm^2))=3.3 10^{-9} A cm^{-2}. The corresponding formal reaction rate, limited by Li diffusion in the solid cathode, may be approximated as k'=4.9 10^{-11} cm^{-1} ($j=k'F$ [Li^+]). In *ac* impedance experiments, the voltage amplitude is very low (10 mV), and the perturbation of Li concentration in the anode is negligible. Hence, the diffusion coefficient D of Li in $LiNiO_2$ may be approximated as $k'\approx D/d$ (where d is the unit length of the diffusion path, d=1 cm): $D\approx 10^{-11}$ cm^2 s^{-1}, which is consistent with literature data [37].

Electrolyte flash point

Flash point of a classical 1 M $LiPF_6$ in EC+DMC (1:1) electrolyte (1.5 ml)+$LiNiO_2$ (5 mg) was measured to be *ca.* 35 °C. This indicates easy ignition of such a classical cathode/electrolyte system. However, if the molecular solvent (EC+DMC) is replaced by an ionic liquid, flash point is considerably increased, and flammability is reduced. The flash point of a 0.7 M $LiNTf_2$ in $MePrPyrrNTf_2$+10% VC (1.5 ml)+$LiNiO_2$ (5 mg) system was determined to be much higher: *ca*. 155 °C. Generally, in laboratory tests, two- and three-electrode cells may be used. With practical batteries, only two electrode cells are applied. In three electrode cells, the volume of the electrolyte is usually relatively high (millilitres or more), while the surface of the working electrode is low (usually the surface of ca. 10^{-2} cm^2 or less). Hence, the amount of SEI forming compound versus the area of the protected lithium surface is also high. However, in the case of two electrode laboratory cells and practical Li-ion cells, the surface of electrodes is large with respect to the volume of the electrolyte contained in the separator (thickness usually of 0.2–0.5 mm). Consequently, the active compound capable of forming a protective coating (here VC) is consumed during SEI formation, and its concentration in the electrolyte after a number of cycles may be regarded as negligible. This may cause a further increase of the flash point, which was estimated to be >250 °C for the system without volatile VC and the cathode (0.7 M $LiNTf_2$+$MePrPyrrNTf_2$). All these suggest that the replacement of a classical electrolyte in molecular liquids (cyclic carbonates) by an electrolyte based on an ionic liquid brings about high increase in cathode/electrolyte non-flammability. A similar observation was found in the case of 1-ethyl-3-methylimidazolium bis(trifluoromethanesulphonyl)imide ($EtMeImNTf_2$) [38]. The ionic liquid was mixed with the quaternary EC+DEC+VC+$LiPF_6$ electrolyte. Flammability was detected by observing the flame on the electrolyte surface. It is concluded that the 40% content of $EtMeImNTf_2$ makes the system non-flammable.

Conclusions

1. The $MePrPyrrNTf_2$ ionic liquid is incapable of protective SEI formation on metallic lithium or lithiated graphite. However, after an addition of VC the protective coating is formed, facilitating possible work of the Li-ion cell.
2. SEM images of pristine electrodes and those taken after electrochemical cycling showed changes which may be interpreted as a result of SEI formation.
3. The charging/discharging capacity of the $LiNiO_2$ cathode in the $MePrPyrrNTf_2$ ionic liquid is between 195 and 170 mAh g^{-1}, depending on the rate. The charging/discharging efficiency of the graphite anode drops after 50 cycles from an initial value of ca. 360 mAh g^{-1} to stabilise at 340 mAh g^{-1}.
4. The replacement of a classical electrolyte in molecular liquids (cyclic carbonates) by an electrolyte based on the $MePrPyrrNTf_2$ ionic liquid brings about highly increased the cathode/electrolyte non-flammability.

Acknowledgements Support of grant DS31-202/10 is gratefully acknowledged.

References

1. Weber A, Blomgren GE (2002) In: van Schalkwijk WA, Scrosati B (eds) Advances in lithium-ion batteries. New York, Kluwer
2. Galinski M, Lewandowski A, Stepniak I (2006) Electrochim Acta 51:5567–5580
3. Lewandowski A, Swiderska-Mocek A (2009) J Power Sources 194:601–609
4. Martha SK, Markevich E, Burgel V, Salitra G, Zinigrad E, Markovsky B, Sclar H, Pramovich Z, Heik O, Aurbach D, Exnar

J, Buqa H, Drezen T, Semrau G, Schmidt M, Kovacheva D, Saliyski N (2009) J Power Sources 189:288–296
5. Scrosati B, Garche J (2010) J Power Sources 195:2419–2430
6. Rebelo LPN, Canongia Lopes JN, Esperanca JMSS, Felipe E (2005) J Phys Chem B 109:6040–6043
7. Earle MJ, Esperanca JMSS, Gilea MA, Lopes JNC, Rebelo LPN, Magee JW, Seddon KR, Widegren JA (2006) Nature 439:831–834
8. Zaitsau DH, Kabo GJ, Strechan AA, Paulechka YU, Tschersich A, Verevkin SP, Heintz A (2006) J Phys Chem A 110:7303–7306
9. Santos LMNBF, Canongia Lopes JN, Coutinho JAP, Esperanca JMSS, Gomes LR, Marrucho IM, Rebelo LPN (2007) J Am Chem Soc 129:284–285
10. Armstrong JP, Hurst C, Jones RG, Licence P, Lovelock KRJ, Satterley CJ, Villar-Garcia IJ (2007) Phys Chem Chem Phys 9:982–990
11. Lewandowski A, Swiderska-Mocek A (2009) Z Phys Chem 223:1427–1435
12. Lewandowski A (2010) J Mol Liq 152:63–65
13. Matsumoto H, Sakaebe H, Tatsumi K, Kikuta M, Ishiko E, Kono M (2006) J Power Sources 160:1308–1313
14. Shin JH, Henderson WA, Scaccia S, Prosini PP, Passerini S (2006) J Power Sources 156:560–566
15. Kim GT, Appetecchi GB, Alessandrini F, Passerini S (2007) J Power Sources 171:861–869
16. Saint J, Best AS, Hollenkamp AF, Kerr J, Shin JH, Doeff MM (2008) J Electrochem Soc 155:A172–A180
17. Lewandowski AP, Hollenkamp AF, Done SW, Best AS (2010) J Power Sources 195:2029–2035
18. Fernicola A, Croce F, Scrosati B, Watanabe T, Ohno H (2007) J Power Sources 174:342–348
19. Guerfi A, Dontigny M, Kobayashi Y, Vijh A, Zaghib K (2009) J Solid State Electrochem 13:1003–1014
20. Lux SF, Schmuck M, Appetecchi GB, Passerini S, Winter M, Balducci A (2009) J Power Sources 192:606–611
21. Lux SF, Schmuck M, Jeong S, Passerini S, Winter M, Balducci A (2010) Int J Energy Res 34:97–106
22. Shin JH, Cairns EJ (2008) J Power Sources 177:537–545
23. Hassoun J, Fernicola A, Navarra MA, Panero S, Scrosati B (2010) J Power Sources 195:574–579
24. Lewandowski A, Swiderska-Mocek A (2009) J Power Sources 194:502–507
25. Scrosati B (1997) In: Vincent CA, Scrosati B (eds) Modern batteries. New York, Arnold
26. Aurbach D (2000) J Power Sources 89:206–218
27. Buqa H, Golob P, Winter M, Besenhard JO (2001) J Power Sources 97–98:122–125
28. Santner HJ, Möller KC, Ivanco J, Ramsey MG, Netzer FP, Yamaguchi S, Besenhard JO, Winter M (2003) J Power Sources 119–121:368–372
29. Yan J, Xia BJ, Su YC, Zhou XC, Zhang J, Zhang XG (2008) Electrochim Acta 53:7069–7078
30. Yan J, Su YC, Xia BJ, Zhang J (2009) Electrochim Acta 54:3538–3542
31. Broussely M, Perton F, Labat J (1993) J Power Sources 43–44:209–216
32. Song MY, Lee R (2002) J Power Sources 111:97–103
33. Sheu SP, Shih IC, Yao CY, Chen JM, Hurng WM (1997) J Power Sources 68:558–560
34. Arai H, Okada S, Ohtsuka H, Ichimura M, Yamaki J (1995) Solid State Ionics 80:261–269
35. Koksbang R, Barker J, Shi H, Saidi MY (1996) Solid State Ionics 84:1–21
36. Fergus JW (2010) J Power Sources 195:939–954
37. Choi YM, Pyun SI, Moon SI, Hyung YE (1998) J Power Sources 72:83–90
38. Guerfi A, Dontigny M, Charest P, Petitclerc M, Lagace M, Vijh A, Zahib K (2010) J Power Sources 195:845–852